Supplementary Materials for

Diversity-oriented combinatory formulation screen for cardiac RNAi therapeutics with polysaccharide framework

Han Gao, Sen Li, Zhengyi Lan, Da Pan, Gonna Somu Naidu, Dan Peer, Hangrong Chen, Ming Ma*, Zehua Liu*, Hélder A. Santos*

*Corresponding author. Email: mma@mail.sic.ac.cn; zehua.liu@helsinki.fi; h.a.santos@umcg.nl

This PDF file includes:

Methods

Materials and reagents

The endosomolytic polymer EEPG was synthesized as previously reported,[1] β-1,3-1,4-glucan (Barley; Low Viscosity) was purchased from Megazyme, other reversible addition fragmentation chain transfer (RAFT) polymerization agents were purchased from Sigma Aldrich. Chitosan (low molecular weight (Mw), high Mw, and Mw = 15k), PEI (Mw = 800 and Mw = 25k), spermine, and deferoxamine were purchased from Sigma Aldrich. Dextran-spermine and Dextran-diaminobutane were obtained as described before.[2, 3] Lipid 2, Lipid 6, Lipid 8, Lipid 10, and Lipid 14 were kindly gifts from Prof. Dan Peer's lab and reported in previous study[4]. Cell-penetrating peptides (K9, KALA, Transportan and Penetratin) are bought from Apeptide Co., Ltd. GAPDH siRNA, scramble siRNA, Cy5-labelled siRNA, and IRF3 siRNA were purchased from GenePharma. The detail information of antibodies was listed in **Table S8**.

Preparation of different cationic species-derived formulations

The preparation of different categories of cationic materials/EEPG paired formulations was performed by an automated microfluidics platform. Briefly, EEPG polymer was dissolved in 1 M sodium hydroxide buffer or Tris-HCL as stock solution in outer phase. Cationic materials in inner phase were dissolved by specific buffers at certain concentrations, the experimental details were showed in **Table S1**. The flow conditions in two phases were kept at 20 mL h^{-1} to precisely control the assembling process of formulations fabrication. The 48-well plate as module of collection system is capable of collecting samples beneath the outlet and further transfer to the online characterization system controlled by a monitoring device.

Nanoparticles characterization

The hydrodynamic diameter was detected by using a Nanolink S901(Linkoptik Instruments Co., Ltd.), equipped with automatic injection, cleaning, and detection modules. Zeta potential measurements were conducted by using a Zetasizer Nano ZS (Malvern). The morphology of nanoparticles was observed by transmission electron microscopy (TEM), a carbon-coated copper TEM grid (Ted Pella) was used for the preparation of nanoparticles. The TEM analysis was conducted by the FEI Tecnai G2 F20 X-TWIN Transmission Electron Microscope (USA).

Cell culture

Human monocyte THP-1 cell line was cultured in RPMI 1640 Medium supplemented with 10% fetal bovine serum and 1% penicillin-streptomycin (complete RPMI 1640 medium). Murine RAW 264.7 cell line was cultured in high glucose Dulbecco's Modified Eagle's Medium with GlutaMAX supplement (ThermoFisher), containing 10% fetal bovine serum and 1% penicillin-streptomycin. Murine bone marrow derived monocytes were isolated from the tibia of C57BL/6 mice and differentiated into M0 macrophages in complete RPMI 1640 medium supplemented with 20 ng mL^{-1} macrophage colony-stimulating factor (M-CSF). Bone marrow derived macrophages (BMDMs) will be collected at day 6 after stimulation. All the cells were cultured in a humidified incubator with 5% CO_2 at 37 °C.

Cytotoxicity study

For cytotoxicity study, cells were pre-seed in 96-well plates at 1×10^4 cells per well. Prior to this, human monocytes THP-1 cells were incubated with complete RPMI-1640 containing 100 ng mL^{-1} of phorbol 12-myristate 13-acetate (PMA) for 24 h to differentiate into M0 macrophages. The cell viability of different cells was detected by cell counting kit-8 (CCK-8) at 48 h after incubating with

representative nanoformulations, the CCK-8 assay was performed according to the manufacture's protocol.

siRNA encapsulation and transfection

The encapsulation efficiency of siRNA loaded in different nanoparticles was quantified by Ribogreen assay as described elsewhere. For *in vitro* transfections, 3×10^5 cells were pre-seeded in 6-well plates, after attachment, cells were incubated with siGAPDH/siNC-encapsulated nanoparticles at a final working concentration of 50 nM siRNA. The whole cell lysates were collected at 48h post-transfection and processed for further analysis.

Western blot analysis

Cells were detached by scraper and lysed with cold RIPA buffer, followed by fully lysed in a FS30D bath sonicator (Thermo Fisher, USA). The total proteins were extracted at 12000 rpm, 4 °C for 5 min and quantified by using BCA Protein Assay Kit (Thermo Fisher, USA). For western blotting analysis, denatured proteins were separated in a 4-12% SDS-polyacrylamide gel electrophoresis, followed by transferring onto a polyvinylidene fluoride (PVDF) membrane, which was pre-activated by methanol. After blocking with EveryBlot Blocking buffer (Bio-Rad) for 5 min, the membranes were further incubated with diluted primary antibodies overnight at 4 °C. At the second day, after washing with 1 × TBST for three times, the membranes were further incubated with corresponding secondary antibodies for 1h at room temperature. The immunoblots signals were detected by Clarity™ Western ECL Substrate (Bio-Rad) and analyzed by ImageJ software.

Computational aided interpretation

Chemical structures for all compounds were prepared by ChemDraw 21.0 (PerkinElmer), and their corresponding simplified molecular-input line-entry

system (SMILES) representations were summarized in **Supplementary Data 1**. Chemical structure of each compound was energy minimized by Open Babel 2.4.0, and the MolDes of each compound were calculated by alvaDesc 2.0, and variable reduction was conducted based on the following scenarios: constant or near constant values, standard deviation less than 0.0001; at least one missing values in one of the molecules; paired correlation larger or equal to 0.95. The calculated MolDes were correlated to binary or continuous observations from experiments as discussed in the manuscript.

For molecular dynamics simulation, one EEPG molecule and one pairing cationic molecule were placed in a 6×6×6 nm water box with periodic boundary conditions containing ~6,800 TIP3P model water molecules and sodium or chloride counter-ions to neutralize the system. To run the simulations, the GROMACS 5.1.1 simulation package was used with the Amber99sb force field. Electrostatics and van der Waals interactions were evaluated in the default cutoff value. Simulation parameters for all the compounds were obtained from SobTop (Version [1.0 (Dev)] Available online: http://Sobereva.com/Soft). The EEPG-cationic compound configurations were energy minimized and annealed from 0 to 370 K at a constant pressure with an annealing rate of 37 K ps^{-1}. The temperature was kept constant for extra 50 ps, followed by decreasing the temperature to 0 K at a constant pressure with an annealing rate of 37 K ps^{-1}. The periodic annealing was conducted for 4 times and the temperature of the final system was further increased to 298 K at a constant pressure with an annealing rate of 29.8 K ps^{-1}, sequentially run for 1 ns under NPT condition. Exchange between adjacent temperature replicas was attempted every 1 ps. The time step of the simulation was 2 fs. The trajectories were saved every 1 ps, yielding a total of 1,000 snapshots for production analysis. Structures were visualized in VMD.

Animals and murine model establishment

Eight to ten-week-old C57BL/6 mice were purchased from The Jackson Laboratory and randomly allocated to different groups, all animal experiments were performed in compliance with the guidelines from the Institutional Animal Care and Use Committee at School of Basic Medical Sciences of Zhejiang University. All mice were maintained in 12 h light/dark cycle at a constant temperature (22 ± 2 °C), supplied with standard lab chow and water *ad libitum*. For the establishment of murine model with myocardial ischemic reperfusion injury (IR), mice were anesthetized with 1.0% to 1.5% of isoflurane gas by mechanical ventilation via a rodent respirator. After performing left thoracotomy, the left anterior descending (LAD) coronary artery visualized by a microscope was ligated with 8-0 silk suture, followed by confirming the presence of myocardial blanching. Mice were then undergoing 50-minute-long LAD artery ischemia followed by reperfusion.

Biodistribution study

The organ/subcellular distribution of GluCARDIA NPs was performed on LAD ligation induced IR mice. Briefly, C57BL/6 mice underwent IR were intravenously (i.v.) injected of 0.8 mg mL^{-1} ICG-Dextran NPs or ICG-GluCARDIA NPs at 24 h post-reperfusion. 8 h post i.v. administration, the mice were euthanatized and the major organs were harvested for real-time fluorescence imaging. The fluorescent signal from each organ was measured with IVIS® Spectrum CT (PerkinElmer, USA) as described elsewhere[5]. For confocal immunofluorescent imaging, 8 h post i.v. administration, mice were euthanatized and hearts were harvest for histologic section. 4',6-diamidino-2-phenylindole (DAPI) was used to stain the nucleus, F4/80 was used to stain the macrophages and Ly-6G was used to stain the neutrophils, the detailed information of corresponding antibodies was listed in Table S8. The confocal images were taken with a Zeiss LSM 780 (Carl Zeiss, Germany) inverted confocal microscope.

In vivo treatment with GluCARDIA NPs

Scrambled siRNA (siNC)/siIRF3-loaded GluCARDIA NPs were i.v. injected to mice at 10 min, day 2, day 4 post-IR injury (siRNA dosage 2.64 μg, 0.1 mg/kg for each injection). At the 1 week and 5 weeks post-IR, the echocardiography imaging analysis was performed to monitor the cardiac function in different groups after i.v. administration. Mice were anesthetized by isoflurane, followed by gently fixing on the echo pad in a supine position. M-mode scanning was conducted as a continuous tracing to show the motion of the myocardial walls as they contract during systole and relax during diastole. The major parameters obtained from M-mode imaging include left eft ventricular end systolic volume (LVESV), left ventricular end diastolic volume (LVEDV) were then used to calculate ejection fraction (EF) to reflect cardiac contractility. The mathematical formula for calculating EF:

$EF = [(LVEDV-LVESV)/LVEDV] \times 100.$

For immunohistological analysis, dissected heart and liver tissues were fixed in 4% paraformaldehyde and embedded in paraffin, followed by processing for tissue-section staining. The detail information of antibodies was showed in **Table S8**.

RNA-sequencing transcriptome analysis

The total cell RNA isolated from heart tissues were extracted using TRLzol Reagent according to the manufacturer's protocol. DNaseI was used to eliminate DNA, followed by analyzed with Agilent 2100 Bioanalyzer to evaluate the purity and integrity of RNA samples. cDNA libraries were prepared by using the NEBNext Ultra Directional RNA Library PrepKit, the NEBNext Poly (A) mRNA Magnetic Isolation Module and NEBNextMultiplex Oligos, which were further tested by Agilent 2100 Bioanalyzer. The final cDNA libraries were established after purification and quantification in ABI StepOnePlus RealTime PCR System. The high-throughput RNA-sequencing was conducted on the Illumina HiSeq.

Statistical analysis

Two-tailed Student's unpaired *t*-test or One-way analysis of variance (AVOVA) followed by Tukey test was conducted to compare between two groups or among different groups. The statistical analysis was performed by using GraphPad Prism (version 9.4.1). Data was presented as mean ± SD, $p < 0.05$ was considered as statistical significance. Independent experiments were conducted with a minimum of triplication each condition for comparison. The representative dataset is indicated in the Figures.

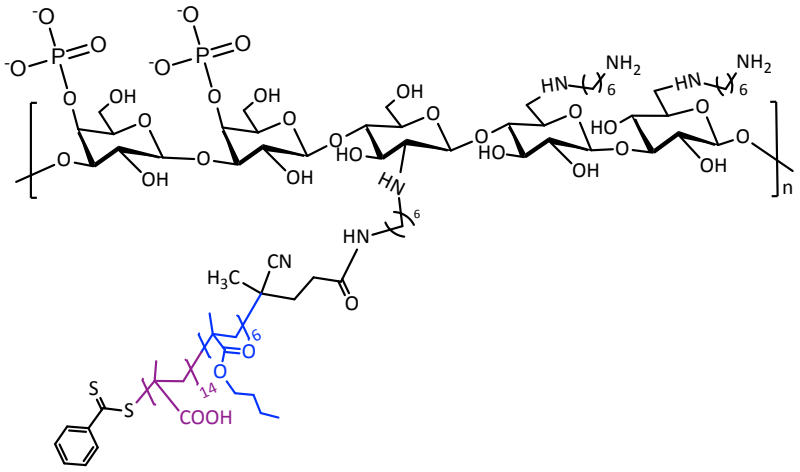

Fig. S1. Structure of endosomolytic phosphorylated β-glucan derivative, EEPG.

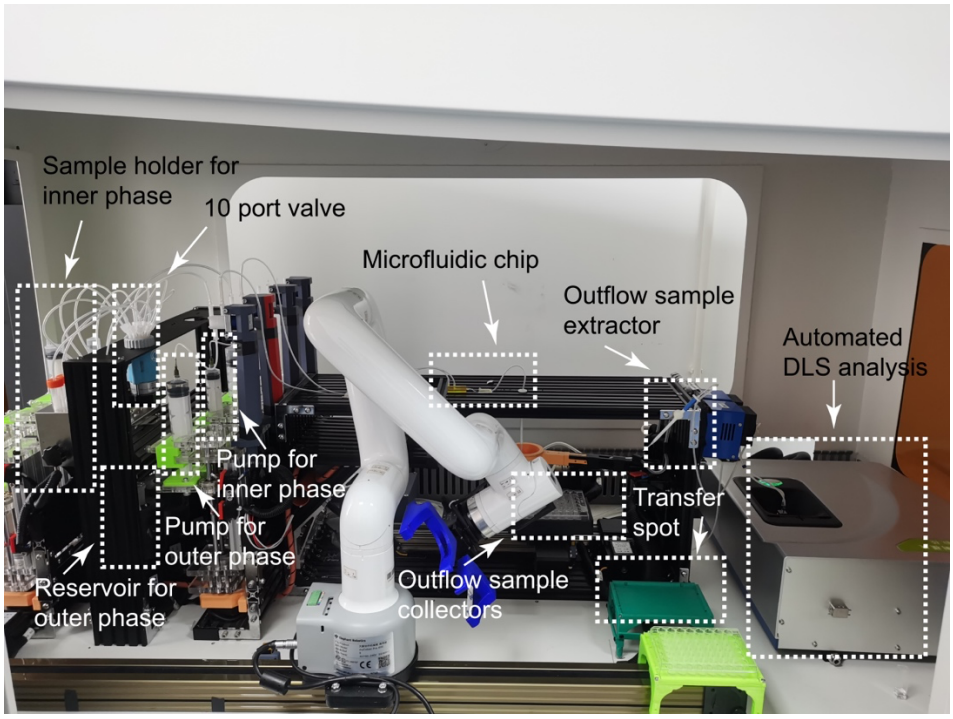

Fig. S2. The representative schematic of the pre-mixed automatic microfluidics system.

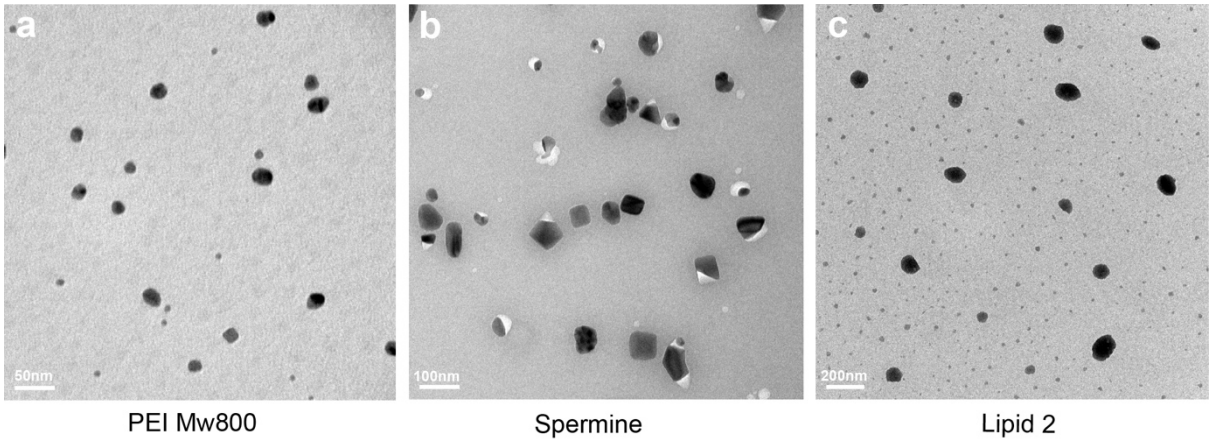

Fig. S3. Representative TEM images from each cationic species-composed nanosystems. (a) PEI (Mw = 800)-EEPG NPs. (b) Spermine-EEPG NPs. (c) Lipid 2-EEPG NPs.

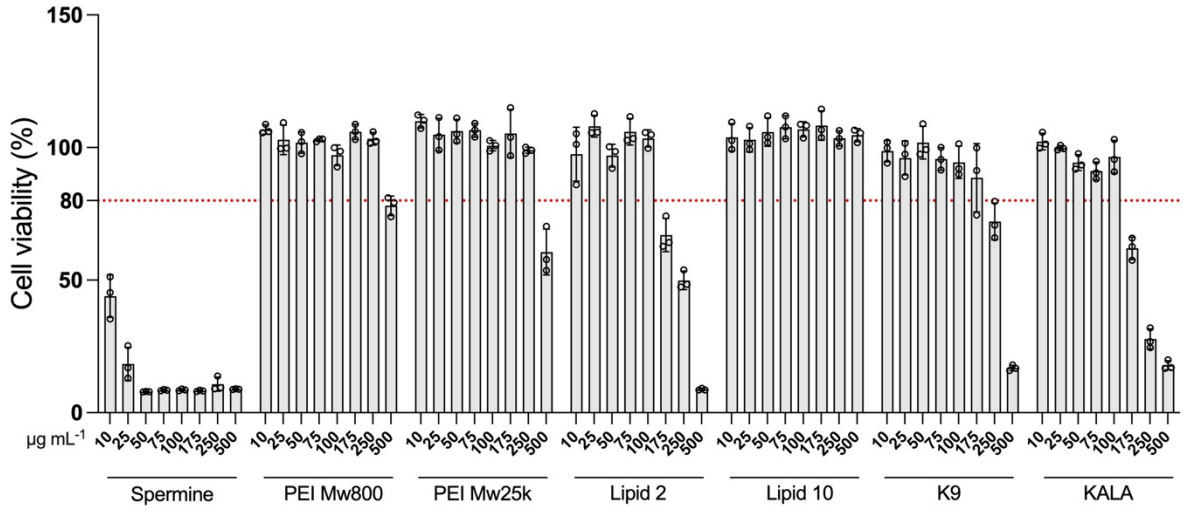

Fig. S4. Cell viability on RAW 264.7 cells after treatment with representative nanosystems for 48 h (n=3 per group). Data are presented as mean ± SD.

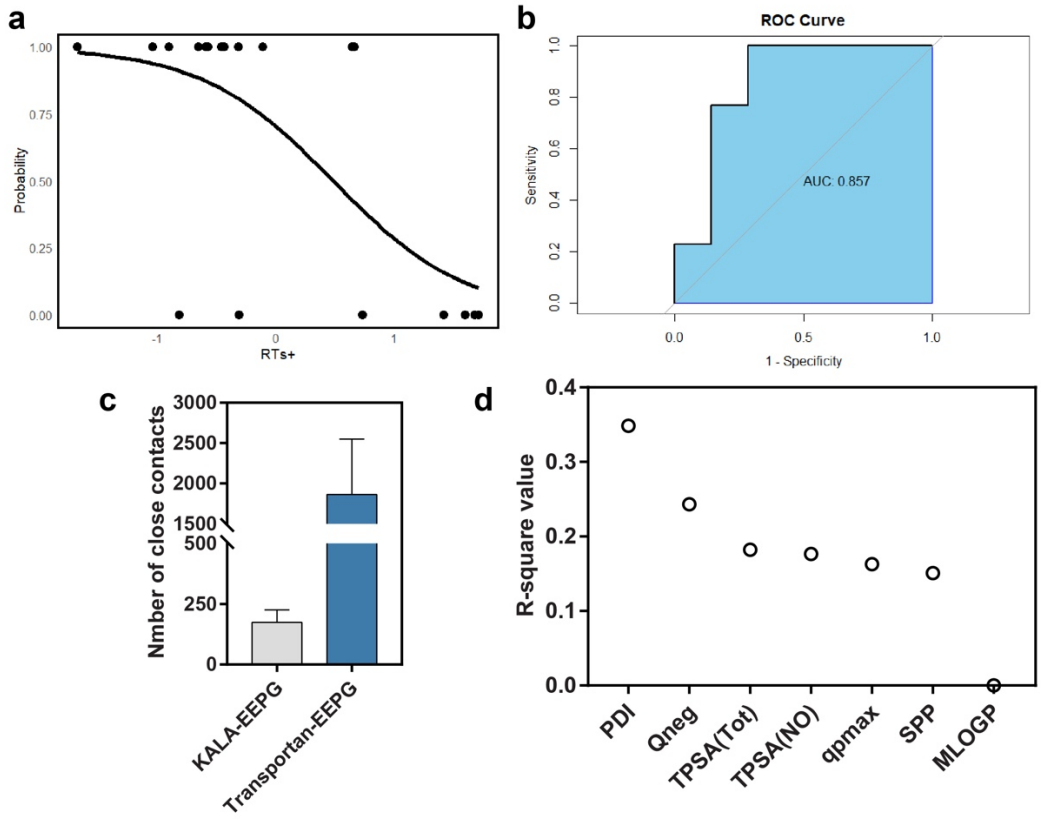

Fig. S5. Computational assisted step-wise interpretation of formulation screening process. (a) RTs+ (R maximal index weighted by intrinsic-state) of MolDes of each cationic compound. (b) The corresponding ROC curve of MolDes with the lowest p-value. (c) Molecular dynamic simulation was performed to compare the number of contacts in KALA-EEPG NPs and Transportan-EEPG NPs. (d) R-square values from MolDes describing hydrophobicity, polar surface area and positive charges.

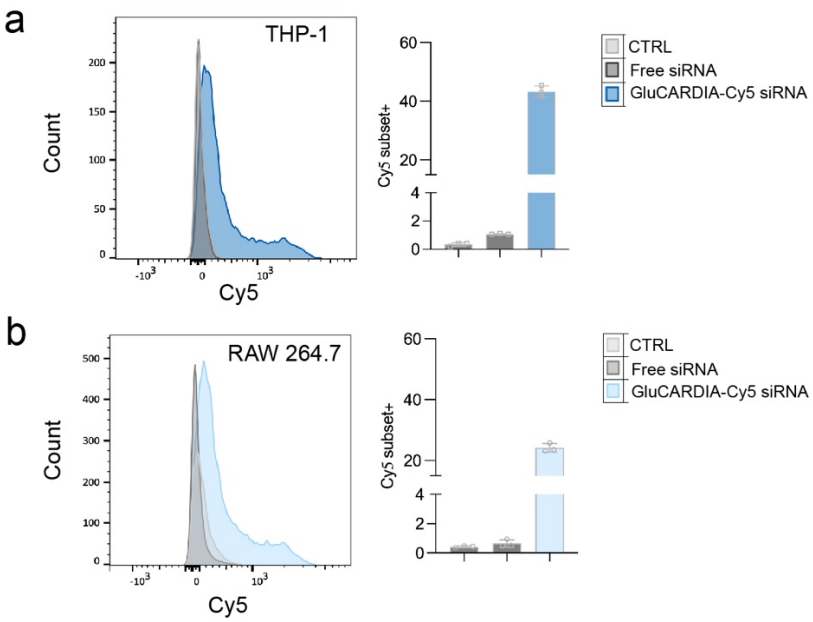

Fig. S6. *In vitro* cellular uptake of GluCARDIA-Cy5 siRNA. (a) Quantitative analysis of Cy5 siRNA uptake in THP-1 cells. (b) Quantitative analysis of Cy5 siRNA uptake in RAW 264.7 cells. Data are presented as mean ± SD.

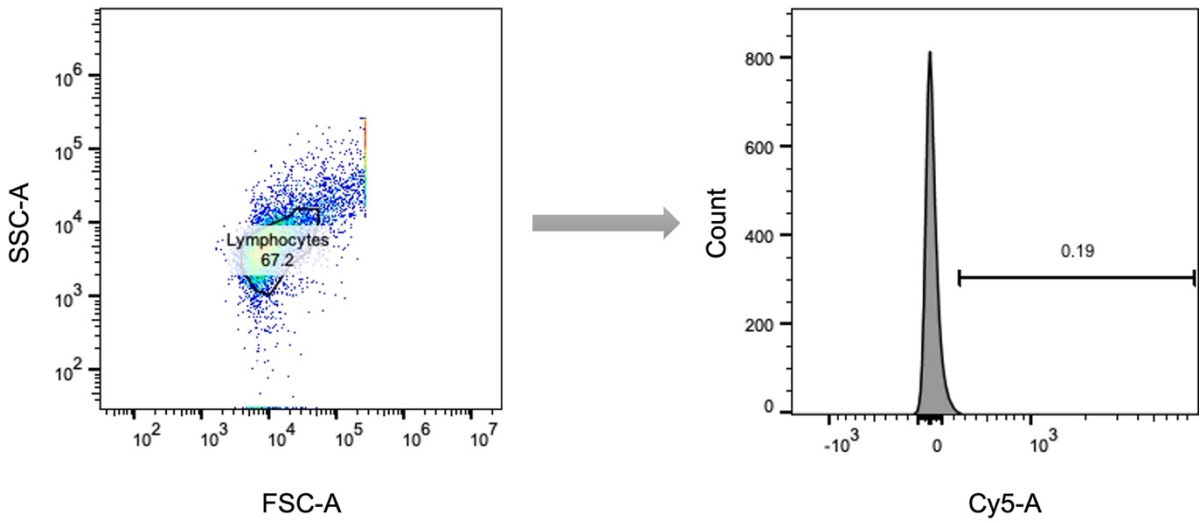

Fig. S7. Flow cytometry gating strategy. Cells were gated to identify Cy5-siRNA signal inside cells.

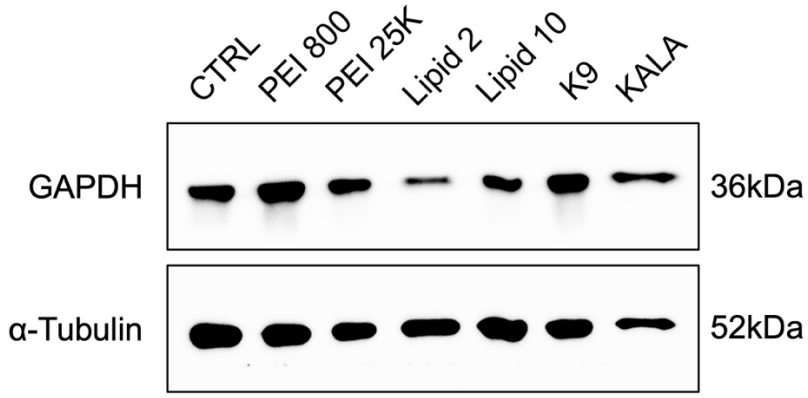

Fig. S8. GAPDH knockdown on RAW 264.7 cells at 48 h post-treatment with representative nanosystems, siGAPDH final concentration at 50 nM (n=3 per group).

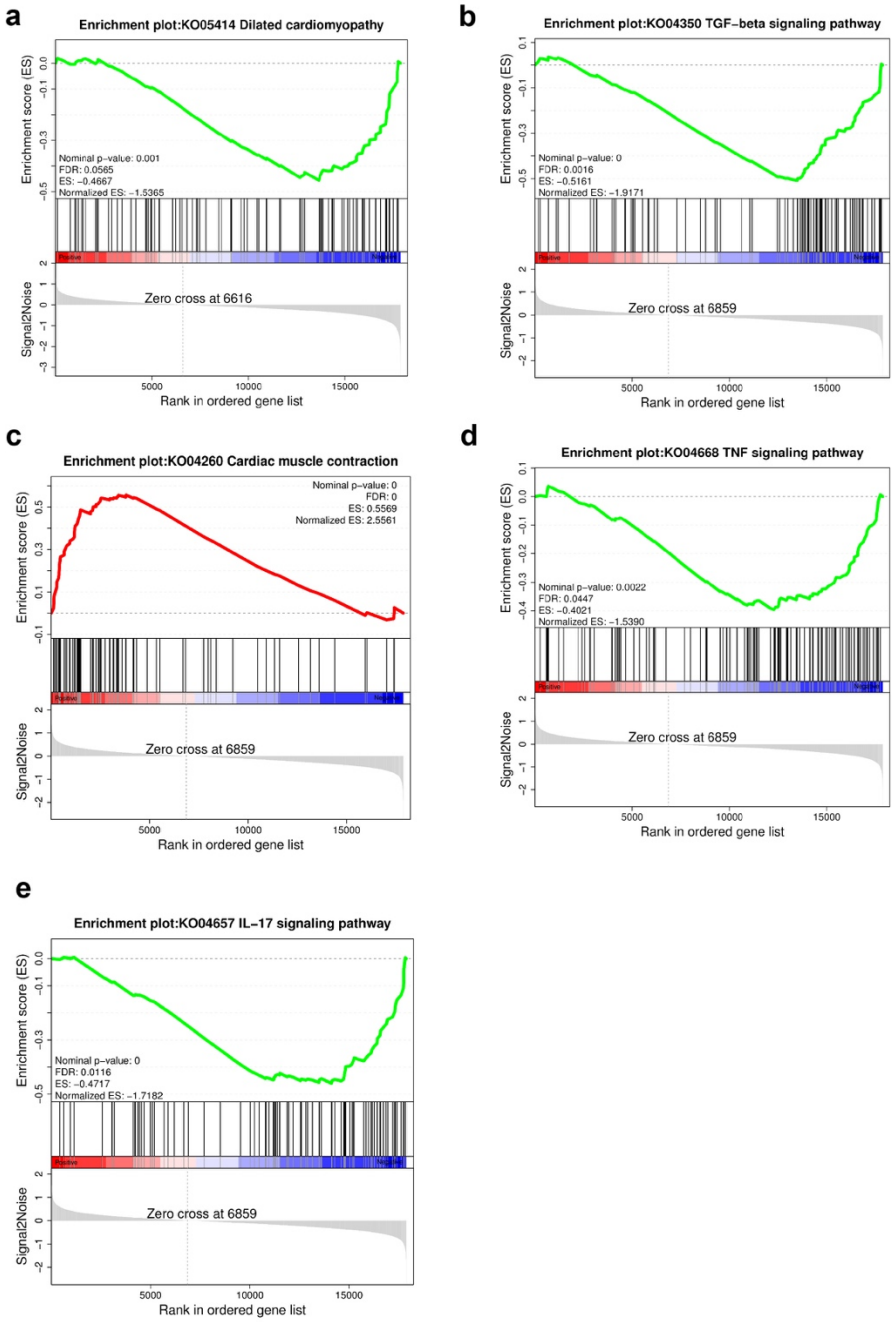

Fig. S9. Gene Set Enrichment Analysis (GSEA) was performed based on the RNA-seq datasets. Positive and negative enrichment score indicate higher and lower expression respectively. (a) IR *vs.* GluCARDIA-siIRF3, negative association between GluCARDIA-siIRF3 treatment and dilated cardiomyopathy was observed. (b) TGF-β pathway analysis, (c) cardiac muscle contraction analysis, (d) TNF pathway analysis, and (e) IL-17 pathway analysis showed GluCARDIA-siIRF3 may inhibited fibrosis progress, promoted cardiac contraction and facilitated the inflammation resolution, comparing to GluCARDIA-siNC group.

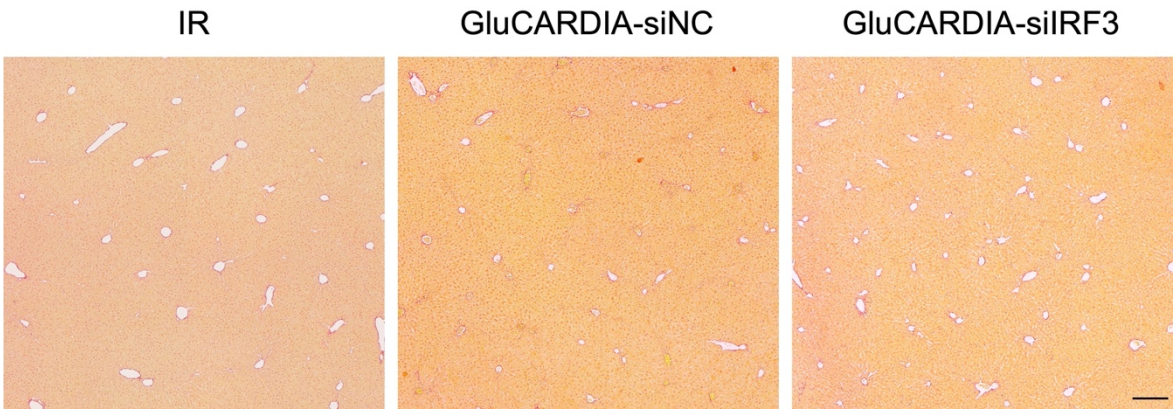

Fig. S10. Representative Sirius Red Staining images of liver sections day 28 post-i.v. injection (n=3 per group). Scale bar: 200 μm.

Table S1. Synthesis conditions for EEPG-focused screen.

Materials ID	**Cationic materials' stock solutions**	**EEPG stock solution**	**Ratios (Cationic materials: EEPG) (range)**	**Flow rates (range)**
#C1 1	0.5 mg mL^{-1} in Tris-HCL	Tris-HCL 0.5 mg mL^{-1}	0.3/1	Inner phase: 20 mL h^{-1} Outer phase: 20 mL h^{-1}
	1mg mL^{-1} in Tris-HCL		0.4/1	
	2mg mL^{-1} in Tris-HCL		0.6/1	
	3mg mL^{-1} in Tris-HCL		0.8/1	
	4mg mL^{-1} in Tris-HCL		1/1	
	5mg mL^{-1} in Tris-HCL		2/1	
	6mg mL^{-1} in Tris-HCL		3/1	
#C1 2	0.5mg mL^{-1} in Tris-HCL	Tris-HCL 0.5 mg mL^{-1}	0.3/1	
	1mg mL^{-1} in Tris-HCL		0.4/1	
	2mg mL^{-1} in Tris-HCL		0.6/1	
	3mg mL^{-1} in Tris-HCL		0.8/1	
	4mg mL^{-1} in Tris-HCL		1/1	
	5mg mL^{-1} in Tris-HCL		2/1	
	6mg mL^{-1} in Tris-HCL		3/1	
#C1 3	0.25mg mL^{-1} in 0.1M HAC	1 M NaOH 1 mg mL^{-1}	0.3/1	
	0.3mg mL^{-1} in 0.1M HAC		0.4/1	
	0.6mg mL^{-1} in 0.1M HAC		0.6/1	
	0.5mg mL^{-1} in 0.1M HAC		0.8/1	
	0.75mg mL^{-1} in 0.1M HAC		1/1	
	1mg mL^{-1} in 0.1M HAC		2/1	
	2mg mL^{-1} in 0.1M HAC		3/1	
#C1 4	0.25mg mL^{-1} in 0.1M HAC	1 M NaOH 1 mg mL^{-1}	0.3/1	
	0.3mg mL^{-1} in 0.1M HAC		0.4/1	
	0.6mg mL^{-1} in 0.1M HAC		0.6/1	
	0.5mg mL^{-1} in 0.1M HAC		0.8/1	
	0.75mg mL^{-1} in 0.1M HAC		1/1	
	1mg mL^{-1} in 0.1M HAC		2/1	
	2mg mL^{-1} in 0.1M HAC		3/1	
#C1 5	0.25mg mL^{-1} in 0.1M HAC	1 M NaOH 1 mg mL^{-1}	0.3/1	
	0.3mg mL^{-1} in 0.1M HAC		0.4/1	
	0.6mg mL^{-1} in 0.1M HAC		0.6/1	
	0.5mg mL^{-1} in 0.1M HAC		0.8/1	
	0.75mg mL^{-1} in 0.1M HAC		1/1	
	1mg mL^{-1} in 0.1M HAC		2/1	
	2mg mL^{-1} in 0.1M HAC		3/1	
#C1 6	0.2mg mL^{-1} in Tris-HCL	Tris-HCL 2 mg mL^{-1}	0.3/1	
	0.25mg mL^{-1} in Tris-HCL		0.4/1	
	0.4mg mL^{-1} in Tris-HCL		0.6/1	
	0.5mg mL^{-1} in Tris-HCL		0.8/1	
	0.67mg mL^{-1} in Tris-HCL		1/1	
	1mg mL^{-1} in Tris-HCL		2/1	
	2mg mL^{-1} in Tris-HCL		3/1	

#C1 7	0.2mg mL^{-1} in Tris-HCL	Tris-HCL 2 mg mL^{-1}	0.3/1	
	0.25mg mL^{-1} in Tris-HCL		0.4/1	
	0.4mg mL^{-1} in Tris-HCL		0.6/1	
	0.5mg mL^{-1} in Tris-HCL		0.8/1	
	0.67mg mL^{-1} in Tris-HCL		1/1	
	1mg mL^{-1} in Tris-HCL		2/1	
	2mg mL^{-1} in Tris-HCL		3/1	
#C2 8	3.2 mg mL^{-1} in 0.1M HAC	1 M NaOH 0.4 mg mL^{-1}	8:1	
	1.6 mg mL^{-1} in 0.1M HAC		4:1	
	1.2 mg mL^{-1} in 0.1M HAC		3:1	
	0.8 mg mL^{-1} in 0.1M HAC		2:1	
	0.4 mg mL^{-1} in 0.1M HAC		1:1	
	0.2 mg mL^{-1} in 0.1M HAC		1:2	
	0.1 mg mL^{-1} in 0.1M HAC		1:4	
#C2 9	3.2 mg mL^{-1} in 0.1M HAC	1 M NaOH 0.4 mg mL^{-1}	8:1	
	1.6 mg mL^{-1} in 0.1M HAC		4:1	
	1.2 mg mL^{-1} in 0.1M HAC		3:1	
	0.8 mg mL^{-1} in 0.1M HAC		2:1	
	0.4 mg mL^{-1} in 0.1M HAC		1:1	
	0.2 mg mL^{-1} in 0.1M HAC		1:2	
	0.1 mg mL^{-1} in 0.1M HAC		1:4	
#C3 10	0.2mg mL^{-1} in Tris-HCL	Tris-HCL 0.4 mg mL^{-1}	1:2	
	0.4mg mL^{-1} in Tris-HCL		1:1	
	0.8mg mL^{-1} in Tris-HCL		2:1	
	1.6mg mL^{-1} in Tris-HCL		4:1	
	3.2mg mL^{-1} in Tris-HCL		8:1	
	4mg mL^{-1} in Tris-HCL		10:1	
	6mg mL^{-1} in Tris-HCL		15:1	
#C3 11	0.2mg mL^{-1} in Tris-HCL	Tris-HCL 0.4 mg mL^{-1}	1:2	
	0.4mg mL^{-1} in Tris-HCL		1:1	
	0.8mg mL^{-1} in Tris-HCL		2:1	
	1.6mg mL^{-1} in Tris-HCL		4:1	
	3.2mg mL^{-1} in Tris-HCL		8:1	
	4mg mL^{-1} in Tris-HCL		10:1	
	6mg mL^{-1} in Tris-HCL		15:1	
#C3 12	0.2mg mL^{-1} in Tris-HCL	Tris-HCL 0.4 mg mL^{-1}	1:2	
	0.4mg mL^{-1} in Tris-HCL		1:1	
	0.8mg mL^{-1} in Tris-HCL		2:1	
	1.6mg mL^{-1} in Tris-HCL		4:1	
	3.2mg mL^{-1} in Tris-HCL		8:1	
	4mg mL^{-1} in Tris-HCL		10:1	
	6mg mL^{-1} in Tris-HCL		15:1	
#C3 13	0.2mg mL^{-1} in Tris-HCL	Tris-HCL 0.4 mg mL^{-1}	1:2	
	0.4mg mL^{-1} in Tris-HCL		1:1	
	0.8mg mL^{-1} in Tris-HCL		2:1	
	1.6mg mL^{-1} in Tris-HCL		4:1	
	3.2mg mL^{-1} in Tris-HCL		8:1	
	4mg mL^{-1} in Tris-HCL		10:1	

	6mg mL^{-1} in Tris-HCL		15:1	
#C4 14	0.1mg mL^{-1} in ETOH:0.1M HAC (v/v 1:3)	1 M NaOH 0.4 mg mL^{-1}	1:4	
	0.1mg mL^{-1} in ETOH:0.1M HAC (v/v 1:3)		1:3	
	0.1mg mL^{-1} in ETOH:0.1M HAC (v/v 1:3)		1:2	
	0.1mg mL^{-1} in ETOH:0.1M HAC (v/v 1:3)		1:1	
	0.1mg mL^{-1} in ETOH:0.1M HAC (v/v 1:3)		2:1	
	0.15mg mL^{-1} in ETOH:0.1M HAC (v/v 1:3)		4:1	
	0.3mg mL^{-1} in ETOH:0.1M HAC (v/v 1:3)		8:1	
#C4 15	0.1mg mL^{-1} in ETOH:0.1M HAC (v/v 1:3)	1 M NaOH 0.4 mg mL^{-1}	1:4	
	0.1mg mL^{-1} in ETOH:0.1M HAC (v/v 1:3)		1:3	
	0.1mg mL^{-1} in ETOH:0.1M HAC (v/v 1:3)		1:2	
	0.1mg mL^{-1} in ETOH:0.1M HAC (v/v 1:3)		1:1	
	0.1mg mL^{-1} in ETOH:0.1M HAC (v/v 1:3)		2:1	
	0.15mg mL^{-1} in ETOH:0.1M HAC (v/v 1:3)		4:1	
	0.3mg mL^{-1} in ETOH:0.1M HAC (v/v 1:3)		8:1	
#C4 16	0.1mg mL^{-1} in ETOH:0.1M HAC (v/v 1:3)	1 M NaOH 0.4 mg mL^{-1}	1:4	
	0.1mg mL^{-1} in ETOH:0.1M HAC (v/v 1:3)		1:3	
	0.1mg mL^{-1} in ETOH:0.1M HAC (v/v 1:3)		1:2	
	0.1mg mL^{-1} in ETOH:0.1M HAC (v/v 1:3)		1:1	
	0.1mg mL^{-1} in ETOH:0.1M HAC (v/v 1:3)		2:1	
	0.15mg mL^{-1} in ETOH:0.1M HAC (v/v 1:3)		4:1	
	0.3mg mL^{-1} in ETOH:0.1M HAC (v/v 1:3)		8:1	
#C4 17	0.1mg mL^{-1} in ETOH:0.1M HAC (v/v 1:3)	1 M NaOH 0.4 mg mL^{-1}	1:4	
	0.1mg mL^{-1} in ETOH:0.1M HAC (v/v 1:3)		1:3	
	0.1mg mL^{-1} in ETOH:0.1M HAC (v/v 1:3)		1:2	

	0.1mg mL^{-1} in ETOH:0.1M HAC (v/v 1:3)		1:1	
	0.1mg mL^{-1} in ETOH:0.1M HAC (v/v 1:3)		2:1	
	0.15mg mL^{-1} in ETOH:0.1M HAC (v/v 1:3)		4:1	
	0.3mg mL^{-1} in ETOH:0.1M HAC (v/v 1:3)		8:1	
#C4 18	0.1mg mL^{-1} in ETOH:0.1M HAC (v/v 1:3)	1 M NaOH 0.4 mg mL^{-1}	1:4	
	0.1mg mL^{-1} in ETOH:0.1M HAC (v/v 1:3)		1:3	
	0.1mg mL^{-1} in ETOH:0.1M HAC (v/v 1:3)		1:2	
	0.1mg mL^{-1} in ETOH:0.1M HAC (v/v 1:3)		1:1	
	0.1mg mL^{-1} in ETOH:0.1M HAC (v/v 1:3)		2:1	
	0.15mg mL^{-1} in ETOH:0.1M HAC (v/v 1:3)		4:1	
	0.3mg mL^{-1} in ETOH:0.1M HAC (v/v 1:3)		8:1	
#C4 19	0.1mg mL^{-1} in ETOH:0.1M HAC (v/v 1:3)	1 M NaOH 0.4 mg mL^{-1}	1:4	
	0.1mg mL^{-1} in ETOH:0.1M HAC (v/v 1:3)		1:3	
	0.1mg mL^{-1} in ETOH:0.1M HAC (v/v 1:3)		1:2	
	0.1mg mL^{-1} in ETOH:0.1M HAC (v/v 1:3)		1:1	
	0.1mg mL^{-1} in ETOH:0.1M HAC (v/v 1:3)		2:1	
	0.15mg mL^{-1} in ETOH:0.1M HAC (v/v 1:3)		4:1	
	0.3mg mL^{-1} in ETOH:0.1M HAC (v/v 1:3)		8:1	
#C4 20	0.1mg mL^{-1} in ETOH:0.1M HAC (v/v 1:3)	1 M NaOH 0.4 mg mL^{-1}	1:4	
	0.1mg mL^{-1} in ETOH:0.1M HAC (v/v 1:3)		1:3	
	0.1mg mL^{-1} in ETOH:0.1M HAC (v/v 1:3)		1:2	
	0.1mg mL^{-1} in ETOH:0.1M HAC (v/v 1:3)		1:1	
	0.1mg mL^{-1} in ETOH:0.1M HAC (v/v 1:3)		2:1	
	0.15mg mL^{-1} in ETOH:0.1M HAC (v/v 1:3)		4:1	

	0.3mg mL^{-1} in ETOH:0.1M HAC (v/v 1:3)		8:1	

*HAC: Sodium acetate buffer; NaOH: sodium hydroxide buffer; Tris-HCL: Tris hydrochloride buffer.

Table S2. Characterization of polymers-assembled formulations.

C1. Polymers							
N:P ratios	**Dex-dia**	**Dex-spermine**	**CS Low Mw**	**CS Med Mw**	**CS Mw 15k**	**PEI Mw 800**	**PEI Mw 25k**
0.3/1	—	—	—	—	—	—	129.23± 1.68
0.4/1	—	—	—	—	—	128.53± 1.31	136.67± 2.93
0.6/1	—	—	—	—	—	104.77 ±2.29	185.07± 0.21
0.8/1	—	—	191.86± 3.71	371.77± 8.80	137.4± 1.59	—	726.90± 20.78
1/1	—	—	—	—	—	—	—
2/1	—	—	206.93± 2.46	161.23± 2.14	—	—	353.27± 34.08
3/1	—	—	—	—	—	—	—

* — represents non-obvious NPs formation between oppositely charged species.

Table S3. Characterization of small molecular drugs-assembled formulations.

C2. Small molecular drugs		
Weight ratios	**Spermine**	**Deferoxamine**
8/1	214.07±14.93	—
4/1	—	—
3/1	—	—
2/1	—	—
1/1	—	—
1/2	—	—
1/4	—	—

* — represents non-obvious NPs formation between oppositely charged species.

Table S4. Characterization of cell-penetrating peptides-assembled formulations.

C3. Cell-penetrating peptides				
Weight ratios	**K9**	**KALA**	**Transportan**	**Penetratin**
1/2	146.30±0.62	117.30±2.69	144.47±3.23	106.80±2.52
1/1	723.95±193.54	132.23±0.61	136.27±1.42	157.30±2.46
2/1	—	—	—	—
4/1	—	—	—	—
8/1	762.07±119.39	113.93±0.06	—	—
10/1	—	—	—	—
15/1	—	—	—	—

* — represents non-obvious NPs formation between oppositely charged species.

Table S5. Characterization of lipids-assembled formulations.

C4. Lipids							
Weight ratios	**Lipid 2**	**Lipid 6**	**Lipid 8**	**Lipid 10**	**Lipid 14**	**DOTAP**	**MC3**
1/4	—	248.13± 6.67	—	—	—	237.00± 4.78	148.53± 3.65
1/3	84.77± 2.12	—	—	—	—	—	—
1/2	154.47± 1.02	710.30± 34.46	—	—	—	214.90± 6.51	146.90± 2.69
1/1	195.2± 3.00	—	—	—	—	—	137.03± 1.74
2/1	178.97± 2.15	290.03± 8.35	—	—	—	213.50± 9.56	513.43± 43.63
4/1	200.83± 4.48	—	—	—	—	—	502.87± 32.01
8/1	213.3± 8.06	—	—	—	—	—	—

* — represents non-obvious NPs formation between oppositely charged species.

Table S6. Characterization of Lipid 8/Lipid 10/Lipid 14-assembled formulations.

C4. Lipids			
Weight ratios	**Lipid 8**	**Lipid 10**	**Lipid 14**
1/35	169.10± 2.80	—	—
1/30	168.57± 2.12	—	—
1/25	184.20± 2.75	166.53± 4.15	—
1/20	214.13± 2.89	—	—
1/15	658.70± 109.24	223.90± 5.65	—
1/10	—	—	—
1/8	—	—	—

* — represents non-obvious NPs formation between oppositely charged species.

Table S7. Dictionary for MolDes.

Name	Category	Description
qnmax	Charge descriptors	Maximum negative charge
B02[O-O]	2D atom pairs	Presence/absence of O – O at topological distance 2
B10[N-N]	2D atom pairs	Presence/absence of N – N at topological distance 10
SPP	Charge descriptors	Submolecular polarity parameter
GATS8i	2D autocorrelations	Geary autocorrelation of lag 8 weighted by ionization potential
qpmax	Charge descriptors	Maximum positive charge
Qpos	Charge descriptors	Total positive charge
pKa	Molecular properties	pKa (strongest base)
MLOGP	Molecular properties	Moriguchi octanol-water partition coeff. (logP)
TDB10P	3D autocorrelations	3D Topological distance based descriptors – lag 10 weighted by polarizability
VE2sign_G	3D matrix-based descriptors	Average coefficient of the last eigenvector from geometrical matrix
E3m	WHIM descriptors	3rd component accessibility directional WHIM index / weighted by mass
VE2_Coulomb	3D matrix-based descriptors	Average coefficient of the last eigenvector (absolute values) from Coulomb matrix
H2p	GETAWAY descriptors	H autocorrelation of lag 2 / weighted by polarizability
PDI	Molecular properties	Packing density index
Qneg	Charge descriptors	Total negative charge
TPSA(Tot)	Molecular properties	Topological polar surface area using N,O,S,P polar contributions
TPSA(NO)	Molecular properties	Topological polar surface area using N,O polar contributions

Table S8. List of antibodies used in this study.

Antibody specificity	Supplier	Cat. No.
GAPDH monoclonal antibody	Proteintech	60004-1-Ig
HRP-conjugated Alpha Tubulin Monoclonal antibody	Proteintech	HRP-66031
IRF3 monoclonal antibody	Proteintech	66670-1-Ig
Phospho-IRF3 (Ser396) antibody	Affinity Biosciences	AF2436
Recombinant mouse Dectin-1	Abcam	ab217331
Ly-6G	R&D Systems	MAB1037
DAPI	Servicebio	G1012
HRP-conjugated Affinipure Goat Anti-Rabbit IgG(H+L)	Proteintech	SA00001-2
HRP-conjugated Affinipure Goat Anti-Mouse IgG(H+L)	Proteintech	SA00001-1

References:

1. Gao H*, et al.* Rational design of a polysaccharide-based viral mimicry nanocomplex for potent gene silencing in inflammatory tissues. *Journal of Controlled Release* **357**, 120-132 (2023).

2. Liu Z*, et al.* Multifunctional Nanohybrid Based on Porous Silicon Nanoparticles, Gold Nanoparticles, and Acetalated Dextran for Liver Regeneration and Acute Liver Failure Theranostics. *Advanced Materials* **30**, 1703393 (2018).

3. Molinaro G*, et al.* In Vitro Study of the Anti-inflammatory and Antifibrotic Activity of Tannic Acid-Coated Curcumin-Loaded Nanoparticles in Human Tenocytes. *ACS Applied Materials & Interfaces* **15**, 23012-23023 (2023).

4. Ramishetti S*, et al.* A Combinatorial Library of Lipid Nanoparticles for RNA Delivery to Leukocytes. *Advanced Materials* **32**, 1906128 (2020).

5. Au - Lim E, Au - Modi KD, Au - Kim J. In vivo Bioluminescent Imaging of Mammary Tumors Using IVIS Spectrum. *JoVE*, e1210 (2009).